Available online at www.sciencedirect.com
SCIENCE DIRECT®
Carbohydrate Research 340 (2005) 2598–2611
Carbohydrate RESEARCH

Complex *O*-acetylation in non-typeable *Haemophilus influenzae* lipopolysaccharide: evidence for a novel site of *O*-acetylation

Håkan H. Yildirim,[a,*] Jianjun Li,[b] James C. Richards,[b] Derek W. Hood,[c] E. Richard Moxon[c] and Elke K. H. Schweda[a]

[a]*Clinical Research Centre, Karolinska Institutet and University College of South Stockholm, NOVUM, S-141 86 Huddinge, Sweden*
[b]*Institute for Biological Sciences, National Research Council of Canada, Ottawa, Ontario, Canada K1A OR6*
[c]*Molecular Infectious Diseases Group and Department of Paediatrics, Weatherall Institute of Molecular Medicine, John Radcliffe Hospital, Oxford OX3 9DS, UK*

Received 9 June 2005; received in revised form 9 August 2005; accepted 7 September 2005
Available online 30 September 2005

Abstract—The structure of the lipopolysaccharide (LPS) of non-typeable *Haemophilus influenzae* strain 723 has been elucidated using NMR spectroscopy and electrospray ionization mass spectrometry (ESI-MS) on *O*-deacylated LPS and core oligosaccharide material (OS), as well as ESI-MS^n on permethylated dephosphorylated OS. It was found that the LPS contains the common structural element of *H. influenzae*, L-α-D-Hep*p*-(1→2)-[*P*Etn→6]-L-α-D-Hep*p*-(1→3)-[β-D-Glc*p*-(1→4)]-L-α-D-Hep*p*-(1→5)-[*PP*Etn→4]-α-Kdo-(2→6)-Lipid A, in which the β-D-Glc*p* residue (GlcI) is substituted by phosphocholine at O-6 and the distal heptose residue (HepIII) by *P*Etn at O-3, respectively. In a subpopulation of glycoforms O-2 of HepIII was substituted by β-D-Gal*p*-(1→4)-β-D-Glc*p*-(1→ or β-D-Glc*p*-(1→. Considerable heterogeneity of the LPS was due to the extent of substitution by *O*-acetyl groups (Ac) and ester-linked glycine of the core oligosaccharide. The location for glycine was found to be at Kdo. Prominent acetylation sites were found to be at GlcI, HepIII, and the proximal heptose (HepI) residue of the triheptosyl moiety. Moreover, GlcI was acetylated at O-3 and/or O-4 and HepI was acetylated at O-2 as evidenced by capillary electrophoresis ESI-MS^n in combination with NMR analyses. This is the first study to show that an acetyl group can substitute HepI of the inner-core region of *H. influenzae* LPS.

Keywords: *Haemophilus influenzae*; Lipopolysaccharide; Acetylation; NMR spectroscopy; Mass spectrometry

1. Introduction

Haemophilus influenzae is an important cause of human disease worldwide and exists in encapsulated (types a through f) and unencapsulated (non-typeable) forms. Type b capsular strains are associated with invasive bacteraemic diseases, including meningitis, epiglottitis, cellulitis, and pneumonia whilst acapsular or non-typeable strains of *H. influenzae* (NTHi) are primary pathogens in otitis media and both acute and chronic lower respiratory tract infections.

LPS is an essential and characteristic surface component of *H. influenzae* and is implicated as a major virulence factor.[1] Extensive structural studies of LPS from *H. influenzae* by us and others have led to the identification of a conserved glucose-substituted triheptosyl inner-core moiety L-α-D-Hep*p*-(1→2)-[*P*Etn→6]-L-α-D-Hep*p*-(1→3)-[β-D-Glcp-(1→4)]-L-α-D-Hep*p* linked to lipid A via 3-deoxy-D-*manno*-oct-2-ulosonic acid (Kdo) 4-phosphate. This inner-core unit provides the template for attachment of oligosaccharide and non-carbohydrate substituents.[2–10] Prominent non-carbohydrate

Abbreviations: CE, capillary electrophoresis; Kdo, 3-deoxy-D-*manno*-oct-2-ulosonic acid; *An*Kdo-ol, reduced anhydro Kdo; Hep, heptose; L,D-Hep, L-*glycero*-D-*manno*-heptose; Hex, hexose; LPS-OH, *O*-deacylated lipopolysaccharide; lipid A-OH, *O*-deacylated lipid A; LPS, lipopolysaccharide; MS^n, multiple step tandem mass spectrometry; NTHi, non-typeable *Haemophilus influenzae*; OS, oligosaccharide; *P*Cho, phosphocholine; *P*Etn, phosphoethanolamine; *PP*Etn, pyrophosphoethanolamine; Ac, acetate; Gly, glycine.

* Corresponding author. Tel.: +46 8 585 838 41; fax: +46 8 585 838 20; e-mail: hakan.yildirim@kfc.ki.se

0008-6215/$ - see front matter © 2005 Elsevier Ltd. All rights reserved.
doi:10.1016/j.carres.2005.09.005

substituents are free phosphate groups (*P*), phosphoethanolamine (*P*Etn), pyrophosphoethanolamine (*PP*Etn), phosphocholine (*P*Cho), acetate (Ac), and glycine (Gly).

LPS of *H. influenzae* can mimic host glycolipids and has a propensity for reversible switching of expression of saccharide and non-carbohydrate epitopes (phase variation) leading to a very heterogeneous population of LPS molecules within a single strain. Phase variation is thought to provide an adaptive mechanism, which is advantageous for the survival of bacteria confronted by the differing microenvironments and immune responses of the host.[11] Our previous studies have focused on the extent of conservation and variability of LPS expression in a representative set of clinical isolates of NTHi obtained from otitis media patients[5,12–15] and relating this to the role of the molecule in commensal and virulence behavior.

In this study, we report on the structural analysis of the LPS from NTHi strain 723, which exhibits novel substitution patterns by acetyl groups in the inner-core region and is the first example of a strain that carries this substituent on HepI.

2. Results

2.1. Isolation and characterization of LPS from 723

The strains were grown in liquid culture and the LPS was isolated by using the phenol/chloroform/light petroleum extraction method.[16] *O*-Deacylation of LPS by treatment with anhydrous hydrazine under mild conditions afforded water-soluble material (LPS-OH). Compositional analysis of the LPS-OH sample 723 identified D-glucose (Glc), D-galactose, 2-amino-2-deoxy-D-glucose (GlcN), and L-*glycero*-D-*manno*-heptose (Hep) as the constituent sugars by GLC–MS analysis of the derived alditol acetates and 2-butyl glycoside derivatives on OS material (Table 1). In earlier investigations it was found that the LPS of 723 contained ester-linked glycine and Neu5Ac as shown by HPAEC-PAD, following treatment of samples with 0.1 M NaOH and neuraminidase, respectively.[17,18]

Table 1. Sugar analysis data for OS derived from dephosphorylated 723 LPS core oligosaccharide and for LPS-OH from 723 and 723-2 batch growths

Sugar residue[a]	Relative detector response (%)		
	723 OS-P	723 LPS-OH	723-2 LPS-OH
Glc	26	9	21
Gal	1	2	8
Hep	72	53	39
GlcNAc		36	32

[a] Sugars were identified by GLC–MS as their alditol acetates.

The ESI-MS spectrum of LPS-OH from 723 revealed abundant molecular peaks corresponding to triply and quadruply deprotonated ions.

The MS data indicated the presence of a heterogeneous mixture of glycoforms in which each molecular species contains the conserved *P*Etn substituted triheptosyl inner-core moiety attached via a phosphorylated Kdo linked to the *O*-deacylated lipid A (lipid A-OH). Moreover, subpopulations of glycoforms were observed, which differed sequentially by 123 Da, indicating LPS substitution with one, two, or three *P*Etn group. Triply charged ions were observed at *m*/*z* 758.7/799.8/840.8, 853.5, and 908.8/948.9, corresponding to the glycoforms *P*Cho·Hex_1·Hep_3·*P*Etn_{1-3}·P_1·Kdo_1·LipidA-OH, *P*Cho·Hex_2·Hep_3·*P*Etn_2·P_1·Kdo_1·LipidA-OH, and *P*Cho·Hex_3·Hep_3·*P*Etn_{2-3}·P_1·Kdo_1·LipidA-OH as shown in Table 2.

2.2. Characterization of oligosaccharides derived from 723

Core OS material was obtained after mild hydrolysis of LPS from 723 (OS723) with dilute aqueous acetic acid and purification by gel filtration chromatography. Part of the material was dephosphorylated with 48% HF to give OS-P. Sugar analysis of OS-P, shown in Table 1, revealed Glc, Gal, and Hep. The absence of GlcN in the OS-P sample confirmed this sugar to be part of Lipid A. Methylation analysis of OS-P revealed major amounts of terminal Glc, terminal Hep, 2-substituted Hep, and 3,4-disubstituted Hep (Table 3). The methylation analysis data were consistent with monoantennary structures, containing the common inner-core element, L-α-D-Hep*p*-(1→2)-L-α-D-Hep*p*-(1→3)-[β-D-Glc*p*-(1→4)]-L-α-D-Hep*p*-(1→5)-α-Kdo*p* of *H. influenzae* LPS.

ESI-MS on the OS723 sample (Table 2) revealed 16 glycoforms in which the heterogeneity was due to the degree of glycosylation (Hex_{1-3}), acetylation (Ac_{0-3}), glycylation (Gly_{0-1}), and/or phosphorylation (*P*Etn_{1-2}). All glycoforms comprised an anhydro-Kdo moiety (*An*-Kdo-ol) formed during delipidation by β-elimination of a *PP*Etn group from C-4 of Kdo as observed in previous studies.[2,19,20] The three most abundant ions were observed at *m*/*z* 684.8, 705.8, and 726.8 corresponding to *P*Cho·Ac_{0-2}·Hex_1·Hep_3·*P*Etn_2·P_1·*An*Kdo-ol, respectively. Ions corresponding to two Hex2 glycoforms with the composition *P*Cho·Ac_{1-2}·Hex_2·Hep_3·*P*Etn_2·P_1·*An*Kdo-ol were observed at *m*/*z* 786.9 and 807.5, respectively. Ions corresponding to Hex3 glycoforms were identified at *m*/*z* 846.8 and 867.8, representing the compositions *P*Cho·Ac_{0-1}·Hex_3·Hep_3·*P*Etn_2·P_1·*An*Kdo-ol, respectively. Furthermore, several ions of glycoforms containing a single glycine residue were identified at *m*/*z* 672.3 and 734.9/755.7 corresponding to *P*Cho·Ac_1·Gly_1·Hex_1·Hep_3·*P*Etn_1·P_1·*An*Kdo-ol and *P*Cho·Ac_{1-2}·Gly_1·Hex_1·Hep_3·*P*Etn_2·P_1·*An*Kdo-ol, respectively.

Table 2. Negative ion ESI-MS data and proposed compositions for *O*-deacylated LPS (LPS-OH) samples of 723 and 723-2 and oligosaccharide (OS) sample of 723

Sample	Observed ions (m/z)			Molecular mass (Da)		Relative abundance (%)		Proposed composition
	$(M-4H)^{4-}$	$(M-3H)^{3-}$	$(M-2H)^{2-}$	Observed	Calculated	723	723-2	
LPS-OH	568.9	758.7		2279.9	2280.0	10	14	*P*Cho·Hex_1·Hep_3·*P*Etn_1·P_1·Kdo_1·LipidA-OH
	599.7	799.8		2402.6	2403.1	37	37	*P*Cho·Hex_1·Hep_3·*P*Etn_2·P_1·Kdo_1·LipidA-OH
	630.4	840.8		2525.5	2526.1	37	26	*P*Cho·Hex_1·Hep_3·*P*Etn_3·P_1·Kdo_1·LipidA-OH
	639.8	853.5		2563.4	2565.2	7	4	*P*Cho·Hex_2·Hep_3·*P*Etn_2·P_1·Kdo_1·LipidA-OH
	680.6	908.8		2727.9	2727.4	6	10	*P*Cho·Hex_3·Hep_3·*P*Etn_2·P_1·Kdo_1·LipidA-OH
	711.4	948.9		2849.7	2850.4	3	9	*P*Cho·Hex_3·Hep_3·*P*Etn_3·P_1·Kdo_1·LipidA-OH
OS			623.3	1248.6	1248.9	1		*P*Cho·Hex_1·Hep_3·*P*Etn_1·P_1·*An*Kdo-ol
			644.3	1290.6	1290.9	3		*P*Cho·Ac_1·Hex_1·Hep_3·*P*Etn_1·P_1·*An*Kdo-ol
			663.4	1328.8	1330.0	2		Ac_2·Hex_2·Hep_3·*P*Etn_1·P_1·*An*Kdo-ol
			665.3	1332.6	1332.9	5		*P*Cho·Ac_2·Hex_1·Hep_3·*P*Etn_1·P_1·*An*Kdo-ol
			672.3	1346.6	13.048	1		*P*Cho·Ac_1·Gly_1·Hex_1·Hep_3·*P*Etn_1·P_1·*An*Kdo-ol
			684.8	1371.6	1372.0	9		*P*Cho·Hex_1·Hep_3·*P*Etn_2·P_1·*An*Kdo-ol
			686.1	1374.2	1374.9	3		*P*Cho·Ac_3·Hex_1·Hep_3·*P*Etn_1·P_1·*An*Kdo-ol
			705.8	1413.6	1414.0	34		*P*Cho·Ac_1·Hex_1·Hep_3·*P*Etn_2·P_1·*An*Kdo-ol
			726.8	1455.6	1456.0	22		*P*Cho·Ac_2·Hex_1·Hep_3·*P*Etn_2·P_1·*An*Kdo-ol
			734.9	1471.8	1471.0	7		*P*Cho·Ac_1·Gly_1·Hex_1·Hep_3·*P*Etn_2·P_1·*An*Kdo-ol
			747.8	1497.6	1498.0	3		*P*Cho·Ac_3·Hex_1·Hep_3·*P*Etn_2·P_1·*An*Kdo-ol
			755.7	1513.4	1513.0	3		*P*Cho·Ac_2·Gly_1·Hex_1·Hep_3·*P*Etn_2·P_1·*An*Kdo-ol
			786.9	1575.8	1576.1	1		*P*Cho·Ac_1·Hex_2·Hep_3·*P*Etn_2·P_1·*An*Kdo-ol
			807.5	1617.0	1618.1	2		*P*Cho·Ac_2·Hex_2·Hep_3·*P*Etn_2·P_1·*An*Kdo-ol
			846.8	1695.6	1696.3	2		*P*Cho·Hex_3·Hep_3·*P*Etn_2·P_1·*An*Kdo-ol
			867.8	1737.6	1738.3	2		*P*Cho·Ac_1·Hex_3·Hep_3·*P*Etn_2·P_1·*An*Kdo-ol

Average mass units were used for calculation of molecular mass values based on proposed composition as follows: Hex, 162.14; Hep, 192.17; Kdo, 220.18; *An*Kdo-ol, 222.18; *P*, 79.98; *P*Etn 123.05; *P*Cho, 165.05; Gly, 57.05; Ac, 42.04; and lipidA-OH 953.02. Relative abundance was estimated from the area of molecular ion peak relative to the total area (expressed as percentage). Peaks representing less than 5% of the base peak intensity are not included in the table.

Table 3. Methylation analysis data of LPS-OH from 723-2 and the dephosphorylated OS sample (OS-P) derived from 723

Methylated sugar[a]	T_{gm}[b]	Linkage assignment	Relative abundance	
			723 OS-P	723-2 LPS-OH[c]
2,3,4,6-Me_4-Glc	1.00	D-Glc*p*-(1-	23	3
2,3,4,6-Me_4-Gal	1.06	D-Gal*p*-(1-	2	9
2,3,6-Me_3-Glc	1.25	-4)-D-Glc*p*-(1-	2	10
2,3,4,6,7-Me_4-Hep	1.43	L,D-Hep*p*-(1-	23	2
3,4,6,7-Me_4-Hep	1.64	-2)-L,D-Hep*p*-(1-	24	7
2,4,6,7-Me_4-Hep	1.69	-3)-L,D-Hep*p*-(1-	1	2
2,6,7-Me_3-Hep	1.76	-3,4)-L,D-Hep*p*-(1-	23	41
4,6,7-Me_3-Hep	1.85	-2,3)-L,D-Hep*p*-(1-	3	6

[a] 2,3,4,6-Me_4-Glc represents 1,5-di-*O*-acetyl-2,3,4,6-tetra-*O*-methyl-D-glucitol-1-d_1, etc.
[b] Retention times (T_{gm}) are reported relative to 2,3,4,6-Me_4-Glc.
[c] Trace amounts of -3)-D-Gal*p*-(1- and -4)-D-Gal*p*-(1- were also detected.

Minor ions corresponding to Hex1 glycoforms with three acetyl groups were detected at m/z 686.1 and 747.8.

Information on the location of *P*Cho, *P*Etn, Gly, and Ac in the OS723 sample was provided by ESI tandem mass spectrometry (MS/MS) in the positive ion mode following on-line separation by capillary electrophoresis (CE). The product ion spectrum obtained from the doubly charged ion at m/z 736 (composition: *P*Cho·Ac_1·Gly_1·Hex_1·Hep_3·*P*Etn_2·*An*Kdo-ol, Fig. 1A) contained marker ions at m/z 280, 328, and 370 corresponding to Gly*An*Kdo-ol, *P*ChoHex, and PChoAcHex. Ions at m/z 1102 and 1156 corresponded to loss of *P*ChoAcHex and Hep*P*Etn, respectively. The product ion spectrum obtained from the doubly charged ion at m/z 749 (composition: *P*Cho·Ac_3·Hex_1·Hep_3·*P*Etn_2·P_1·*An*Kdo-ol, Fig. 1B) contained the ion at m/z 370 to which additions of AcHep (m/z 604) and *An*Kdo-ol (m/z 826) could be seen. In addition, the ion at m/z 358 corresponded to AcHep*P*Etn to which the addition of Hep*P*Etn gave m/z 673. An ion at m/z 1141 corresponded to the loss of AcHep*P*Etn verifying that acetylation occurred at

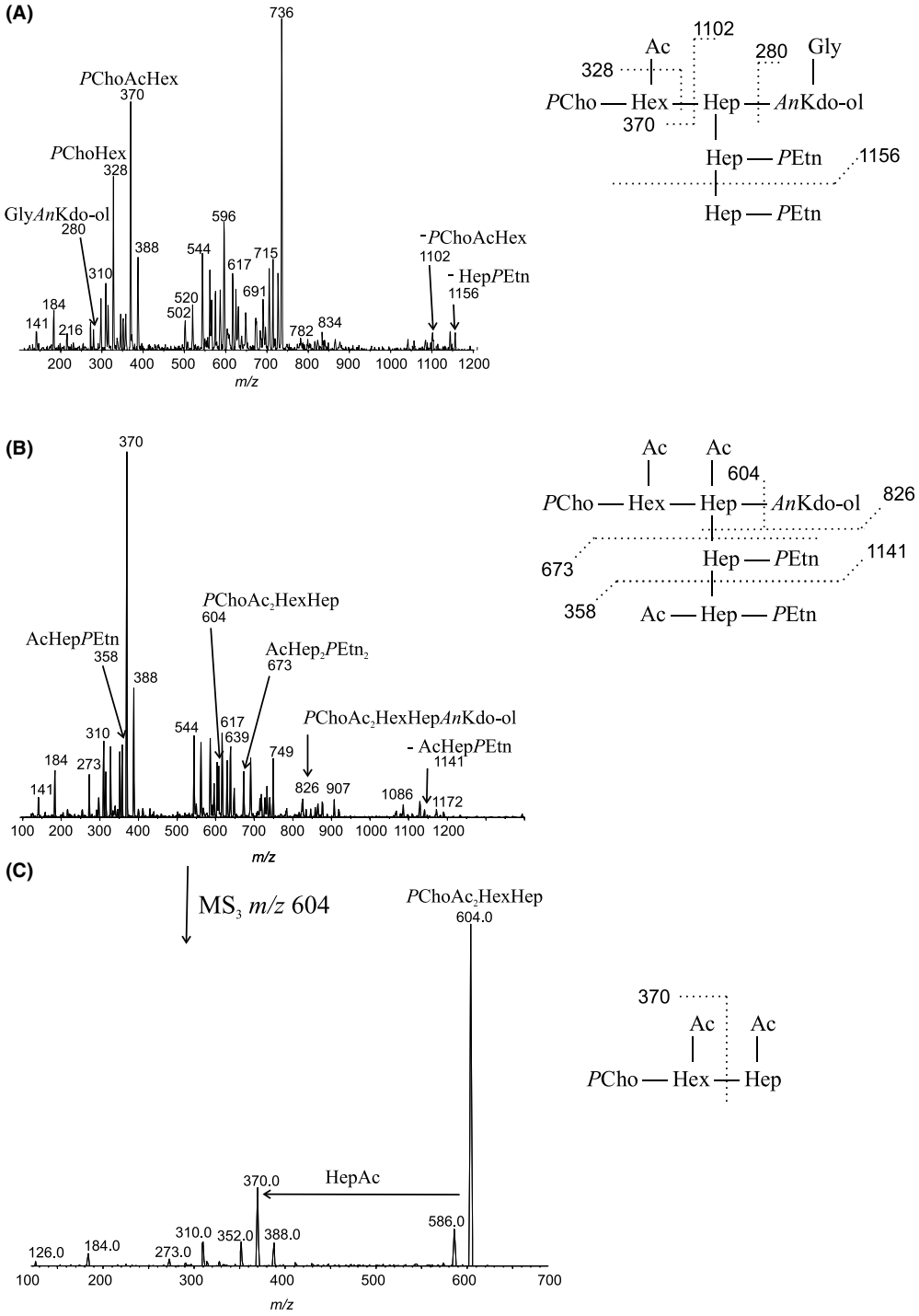

Figure 1. (A) MS^2 spectrum of the doubly charged ion *m*/*z* 736 corresponding to *P*Cho·Ac_1·Gly_1·Hex_1·Hep_3·*P*Etn_2·*An*Kdo-ol. (B) MS^2 spectrum of the doubly charged ion *m*/*z* 749 corresponding to *P*Cho·Ac_3·Hex_1·Hep_3·*P*Etn_2·P_1·*An*Kdo-ol. (C) MS^3 spectrum of *m*/*z* 604. Only ions of significance are indicated in (A), (B), and (C).

HepIII. The ion at *m*/*z* 604 was further fragmented in an MS^3 experiment (Fig. 1C). The product ion at *m*/*z* 370 due to the loss of HepAc provided unambiguous evidence that HepI was acetylated. Furthermore, it was evidenced that *P*Cho substituted GlcI and *P*Etn substituted HepII and HepIII.

2.2.1. Sequence analysis of dephosphorylated and permethylated oligosaccharide samples by multiple step MS (MS^n). OS723 was dephosphorylated, permethylated, and analyzed by ESI-MS^n in order to determine the sequence and branching details of the various glycoforms. The resulting glycoforms are displayed in Table

Table 4. Structures of the glycoforms identified in dephosphorylated and permethylated OS sample derived from 723

Hex1 (93%)	Hex2 (2%)	Hex2 (trace)	Hex3 (5%)
Hex—Hep—AnKdo-ol | Hep | Hep	Hex—Hep—AnKdo-ol | Hep | Hex—Hep	Hep—AnKdo-ol | Hep | Hex—Hex—Hep	Hex—Hep—AnKdo-ol | Hep | Hex—Hex—Hep

4. In the ESI-MS spectrum of OS723 (positive mode) three sodiated adduct ions ([M+Na$^+$]) were observed at *m*/*z* 1263.6 (major), 1468.7, and 1672.5 corresponding to dephosphorylated and permethylated Hex$_{1-3}$-Hep$_3$-*An*Kdo-ol (Fig. 2A). The MS^2 fragmentation of the molecular ion at *m*/*z* 1263.6 resulted in ions at *m*/*z* 1045.4, 1001.4, 753.3, and 533.2 corresponding to neutral loss of tHex, tHepIII, tHepIII-HepII-, and tHex-HepI-*An*Kdo-ol, respectively, suggesting a single structure with a hexose linked to HepI. This was further evidenced by performing MS^3 on *m*/*z* 1001.4 (corresponding to loss of tHepIII), which resulted in a spectrum with ions at *m*/*z* 783.2 and 753.3 corresponding to the neutral loss of -HepII- and tHex, respectively. MS^2 on the molecular ion at *m*/*z* 1468.7 indicated the presence of two Hex2 isomers since ions corresponding to the loss of tHex-HepIII and tHex-Hex-HepIII were detected at *m*/*z* 1001.4 and 797.2, respectively. The spectrum resulting from MS^3 on *m*/*z* 1001.4 showed an ion at *m*/*z* 753.2 corresponding to the loss of -HepII- and hence evidencing a structure with a hexose linked to HepIII and HepI. The second isomer with a disaccharide group attached to HepIII was evidenced by MS^3 spectrum of *m*/*z* 797.2, which showed an ion at *m*/*z* 549.0 representing the loss of -HepII-. The single Hex3 glycoform was determined by performing MS^2 on *m*/*z* 1672.5, which resulted in an ion at *m*/*z* 1001.4 corresponding to the loss of tHex-Hex-HepIII (Fig. 2B). The following MS^3 fragmentation on *m*/*z* 1001.4 gave rise to an ion at *m*/*z* 753.3 corresponding to the loss of -HepII- and evidenced a structure with a disaccharide unit linked to HepIII and a hexose attached to HepI (Fig. 2C).

2.3. NMR spectroscopy on LPS-OH and OS samples

The ^{1}H and ^{13}C NMR resonances of LPS-OH and OS samples were assigned using gradient chemical shift correlation techniques (COSY, phase-sensitive TOCSY, HMQC, phase-sensitive HSQC, and HMBC experiments). The chemical shift data are given in Tables 5 and 6. Subspectra corresponding to the individual glycosyl residues were identified on the basis of spin-connectivity pathways delineated in the ^{1}H chemical shift correlation maps, the chemical shift values, and the vicinal coupling constants.

The chemical shift data are consistent with each D-sugar residue being present in the pyranosyl ring form. Further evidence for this conclusion was obtained from NOE data, which also served to confirm the anomeric configurations of the linkages and the monosaccharide sequence. The Hep ring systems were identified on the basis of the small $J_{1,2}$ values and their α-configurations were confirmed by the occurrence of single intraresidue NOE between the respective H-1 and H-2 resonances.

In the COSY and TOCSY spectra obtained from OS material, several signals for methylene protons of *An*Kdo-ol were observed due to the fact that several anhydro-forms of Kdo are formed during the hydrolysis by elimination of phosphate or pyrophosphoethanolamine from the C-4 position.[19]

2.3.1. LPS-OH from 723. In the NMR spectra of the 723 LPS-OH sample, anomeric ^{1}H/^{13}C NMR resonances of HepI, HepII, and HepIII were identified at δ 5.18/100.7, 5.80/99.3, and 5.21/101.9, respectively. The anomeric signals corresponding to GlcI were observed at δ 4.54/104.0. In addition, the anomeric signals of the α- and β-linked GlcN residues of the lipid A part were observed at δ 5.49/94.6 and 4.63/103.1, respectively. The occurrence of interresidue NOESY connectivities between the proton pairs HepII H-1/HepIII H-1, HepII H-1/HepI H-3, and GlcI H-1/HepI H-4/H-6 confirmed the sequence of the glucose-substituted triheptosyl inner-core moiety L-α-D-Hep*p*-(1→2)-L-α-D-Hep*p*-(1→3)-[β-D-Glc*p*-(1→4)]-L-α-D-Hep*p*. Moreover, a weak NOE signal was observed between HepII H-1 and an anomeric signal at δ 5.18, which indicated a second HepIII spin system. H-2 of this residue was observed at δ 4.08, indicative of an un-phosphorylated HepIII, which is consistent with the ESI-MS data on the oligosaccharide sample indicating that a majority of the glycoforms had two Hep substituted *P*Etn residues while the remaining glycoforms had only one (Table 2).

^{1}H–^{31}P correlation studies were used to identify the linkage positions of *P*EtnI, *P*EtnII, and *P*Cho (Fig. 3). In the ^{1}H–^{31}P HMQC spectrum, a ^{31}P resonance at δ 0.54 coupled to the methylene protons of *P*EtnI at δ 4.14 and to H-6 of HepII at δ 4.56. Moreover, it was determined that *P*EtnII substituted the O-3 position of HepIII since a ^{31}P resonance at δ −0.22 correlated to

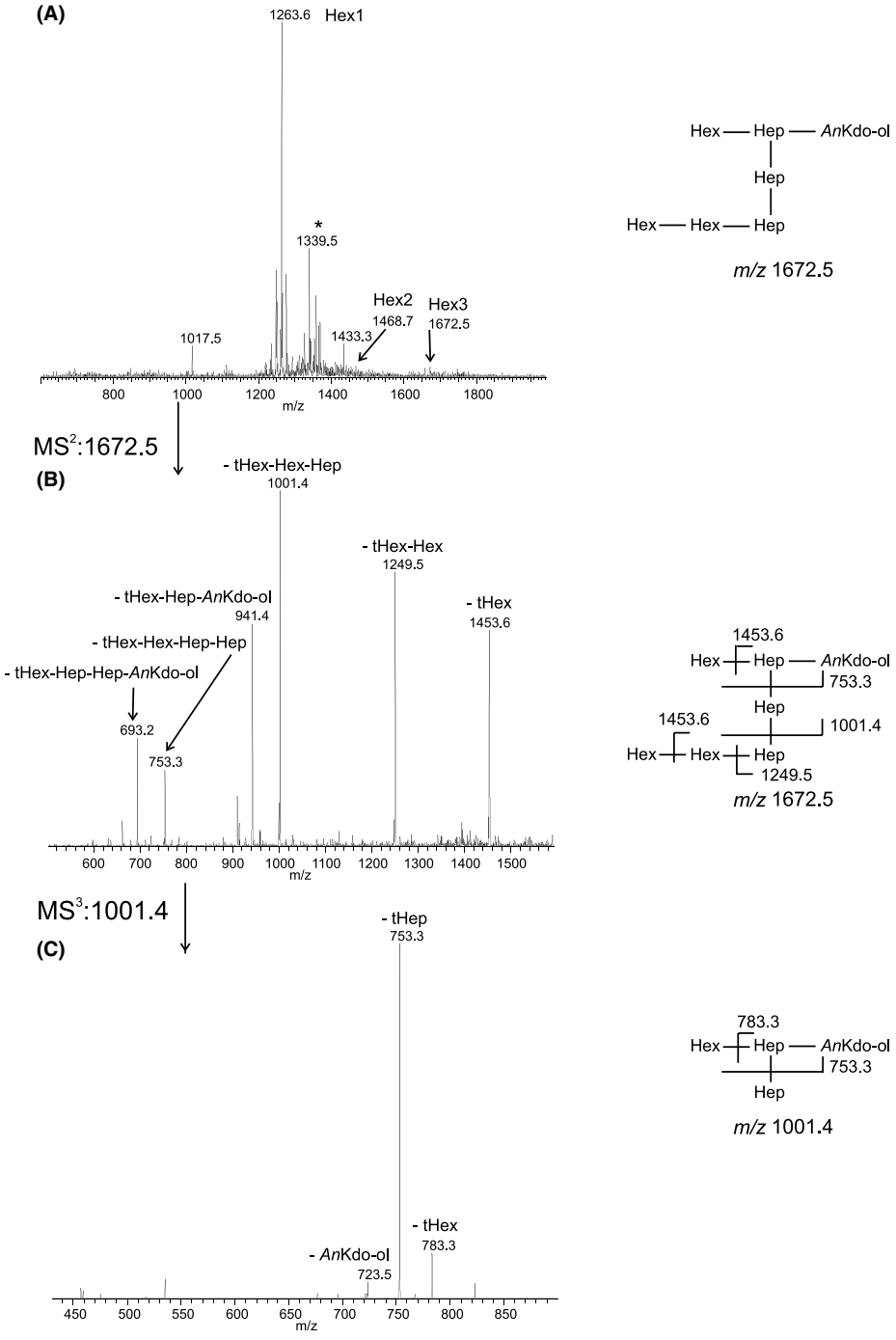

Figure 2. (A) ESI-MS spectrum showing sodiated adducts $[M+Na^+]^+$ of permethylated OS723. The peak denoted with asterisks indicates a glycoform with monomethylated phosphate group resulting from incomplete dephosphorylation. (B) MS^2 spectrum of *m/z* 1672.5. (B) MS^3 spectrum of the fragment ion at *m/z* 1001.4.

the methylene protons of *P*EtnII at δ 4.19 and H-3 of HepIII at δ 4.32. This finding was corroborated by the significantly downfield-shifted H-3 and C-3 of HepIII. The C-3 chemical shift of HepIII was detected in the ^1H–^{13}C HMBC spectrum, which appeared as a intraresidue cross-peak between H-1 and C-3 of HepIII. The ^1H–^{13}C resonances of HepIII could also be identified in the ^1H–^{13}C HMQC spectrum at δ 4.32/76.8. In addition, the downfield-shifted H-$6_{a,b}$ and C-6, and a ^{31}P resonance at δ 0.63 coupled to the methylene protons of *P*Cho and H-$6_{a,b}$ GlcI, provided evidence that this residue was substituted with *P*Cho at O-6. From the combined MS and NMR data it could thus be concluded that the Hex1 glycoform of LPS-OH from 723 has structure 2.

Table 5. ^{1}H and ^{13}C NMR chemical shifts for *O*-deacylated LPS from 723 and 723-2 were recorded in D_2O containing 2 mM perdeutero-EDTA and 10 mg/ml perdeutero-SDS at 22 °C

Residue	Glycose unit		H-1/C-1	H-2/C-2	H-3/C-3	H-4/C-4	H-5/C-5	H-6_A/C-6	H-6_B	H-7_A/C-7	H-7_B
Hex1 glycoform derived from NTHi 723											
GlcNI	→6)-α-D-Glc*p*N(1→		5.49	3.86	—[a]	—[a]	—[a]	—[a]	—[a]		
			94.6	55.7							
GlcNII	→6)-β-D-Glc*p*N(1→		4.63	3.90	—[a]	—[a]	—[a]	—[a]	—[a]		
			103.1	55.7							
HepI	→3, 4)-L-α-D-Hep*p*-(1→	**I**	5.18[b] (n.r.)	4.16[c]	4.08	4.25	—[a]	4.07		—[a]	—[a]
			100.7	70.9[d]	72.4	72.5		70.3			
HepII	→2)-L-α-D-Hep*p*(1→	**II**	5.80 (n.r.)	4.27	—[a]	—[a]	3.69	4.56		3.86	3.94
	6 ↑ *P*Etn		99.3	80.1			70.4[e]	74.8		62.5	
HepIII	L-α-D-Hep*p*(1→ 3 ↑ *P*Etn	**III**	5.21 (n.r.)	4.28	4.32	3.87	4.02	—[a]		—[a]	—[a]
			101.9	74.5	76.8	66.5	72.5				
HepIII	L-α-D-Hep*p*-(1→	**III**	5.18 (n.r.)	4.08[f]	—[a]	—[a]	—[a]	—[a]	—[a]		
			100.7	69.3[g]							
GlcI	*P*Cho→6)-β-D-Glc*p*-(1→	**IV**	4.54 (7.7)	3.46	3.47	3.51	3.56	4.30	4.30		
			104.0	74.3	76.7	70.1	75.4	65.3			
Hex3 glycoform derived from NTHi 723-2											
HepIII	L-α-D-Hep*p*(1→ 3 ↑ *P*Etn	**III**	5.10 (n.r)	4.38	—[a]	—[a]	—[a]	—[a]		—[a]	—[a]
			100.7	76.9							
GlcII	4)-β-D-Glc*p*-(1→	**V**	4.68 (7.8)	3.40	3.67	3.69	3.59	3.99	3.83		
			103.9	73.6	74.7	79.4	74.9	62.7			
GlcI	β-D-Glc*p*-(1→	**VI**	4.45 (8.2)	3.54	3.67	3.93	3.73	—[a]	—[a]		
			104.0	71.8	72.6	69.3	76.3				
*P*EtnI			4.14	3.31							
			62.7	40.7							
*P*EtnII			4.19	3.32							
			62.7	40.7							
*P*Cho			4.39	3.71							
			60.3	66.8							

$^{3}J_{H,H}$ values for anomeric ^{1}H resonances are given in parenthesis; n.r., not resolved (small coupling). Signals corresponding to *P*Cho methyl protons and carbons occurred at 3.25 and 54.8 ppm, respectively.

Chemical shift values, which differ by more than ±0.05 ppm (^{1}H) and 0.5 ppm (^{13}C) between NTHi 723 and 723-2 are denoted with superscript values as follows:

[a] Not determined.

[b] 5.04–5.07.

[c] 4.08–4.10.

[d] 69.3.

[e] 71.9.

[f] 4.17.

[g] 71.0.

Table 6. ^{1}H and ^{13}C NMR chemical shifts for OS derived from 723 (Spectra were recorded in D_2O at 22 °C)

Residue	Glycose unit		H-1/C-1	H-2/C-2	H-3/C-3	H-4/C-4	H-5/C-5	H-6_A/C-6	H-6_B	H-7_A/C-7	H-7_B
HepI	→3, 4)-L-α-D-Hep*p*-(1→	**I**	5.15–5.04 (n.r) 101.1–100.8	4.05–4.00	—[a]	—[a]	—[a]	—[a]		—[a]	
HepI	→3, 4)-L-α-D-Hep*p*(1→ 2 ↑ Ac	**I**	5.08 (n.r.) 99.3 5.08 99.3	5.33 72.3 5.44 71.8	4.50 70.0 4.47 69.3	4.03 —[a] 4.10 —[a]	—[a] —[a]	—[a] —[a]		—[a] —[a]	
HepII	→2)-L-α-D-Hep*p*(1→ 6 ↑ *P*Etn	**II**	5.90–5.72 (n.r) 101.9	4.22–4.31 80.1	—[a]	—[a]	—[a]	—[a]		—[a]	
HepIII	L-α-D-Hep*p*(1→ 3 ↑ *P*Etn	**III**	5.32–5.19 (n.r) 102.0–102.2	4.29–4.27 70.3	4.32 74.3	—[a]	—[a]	—[a]		—[a]	
GlcI	*P*cho→6)-β-D-Glc*p*-(1→	**IV**	4.54 (7.7) 104.0	3.49 74.4	3.58 75.2	3.57 69.9	3.57 75.2	4.27 65.4	4.27		
GlcI	*P*Cho →6)-β-D-Glc*p* (1→ 3 ↑ Ac	**IV**	4.64 (7.7) 104.0 4.60 (7.7) 104.0	3.58 72.5 3.61 72.5	5.04 78.0 5.05 78.0	3.79 67.7 3.82 67.0	3.68 74.6 3.62 74.7	4.22 65.4 4.40 64.8	4.29 4.40		
GlcI	*P*Cho →6)-β-D-Glc*p* (1→ 4 ↑ Ac	**IV**	4.59 (7.8) 104.0	3.50 76.9	3.78 74.7	4.74 72.1	3.78 72.5	4.12 65.4	4.20		
*P*EtnI			4.21–4.16 62.7	3.32–3.30 40.8							
*P*EtnII			4.21–4.16 62.7								
*P*Cho			4.38 60.4	3.71 66.7							

$^{3}J_{H,H}$ values for anomeric ^{1}H resonances are given in parenthesis; n.r., not resolved (small coupling). Signals corresponding to *P*Cho methyl protons and carbons occurred at 3.26 and 54.8 ppm, respectively. Pairs of deoxy protons of reduced, *An*Kdo were identified in the DQF-COSY at δ 1.89–2.16.

[a] Not determined.

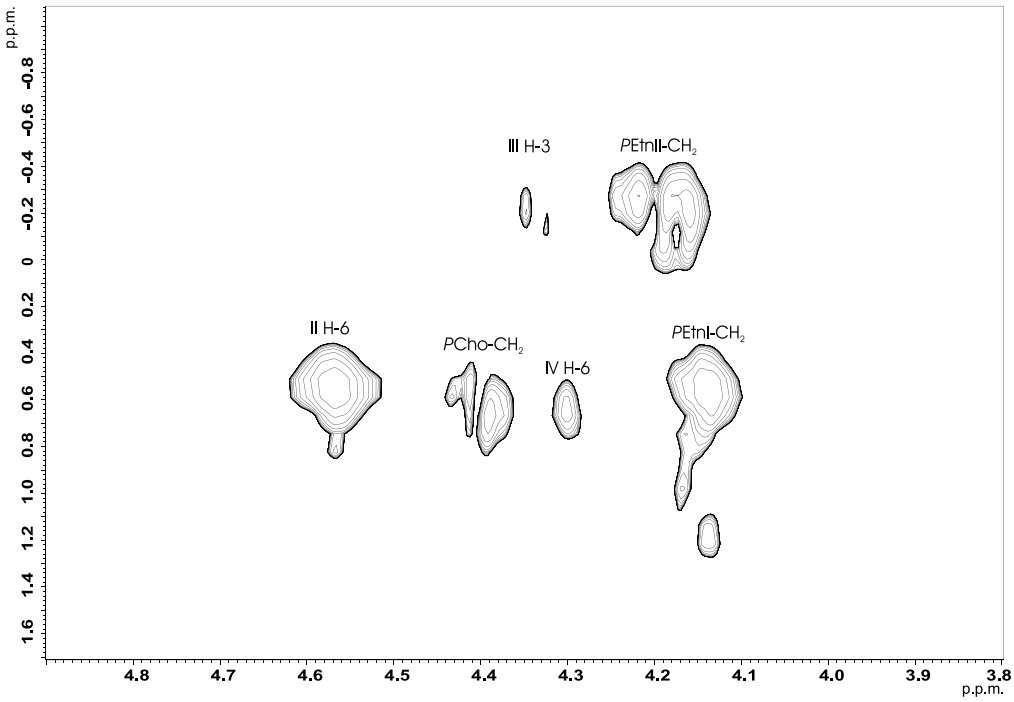

Figure 3. Selected region of the two-dimensional ^{1}H–^{31}P HMQC spectrum of LPS-OH derived from LPS of 723. Cross-peaks of significant importance are labeled. See Table 5 for an explanation of the roman numerals.

*P*Cho *PP*Etn
↓ ↓
6 4
β-D-Glc*p* (1→4)-L-α-D-Hep*p*(1→5)-α-Kdo-LipidA
3
↑
1
L-α-D-Hep*p*6←*P*Etn
2
↑
1
L-α-D-Hep*p*3←*P*Etn

Structure 2

2.3.2. OS from 723. The ESI-MS data of OS723 evidenced that the most abundant glycoform in this strain was monoacetylated and the second most abundant glycoform was diacetylated. Also, by CE-ESI-MS/MS acetylation sites were found at GlcI, HepI, and HepIII. The heterogeneity due to acetylation in the OS material was apparent in the NMR spectrum of OS723 with several overlapping signals and the multiple acetylation sites. In the TOCSY spectrum, the anomeric signal of a non-acetylated GlcI spin system was identified at δ 4.54 (Table 6, Fig. 4). Moreover, a minor H-1 signal of a spin system belonging to GlcI acetylated at O-4 position ($GlcI^{4\text{-}OAc}$) was identified at δ 4.59. This observation was based on downfield-shifted signals from H-3 (0.20 ppm), H-4 (1.17 ppm), H-5 (0.21 ppm), and C-4 (2.2 ppm), while the resonances for C-3 (−0.5 ppm), and C-5 (−2.7 ppm) were shifted upfield compared with the non-acetylated residue. Furthermore, two major spin systems corresponding to GlcI residues acetylated at position O-3 ($GlcI^{3\text{-}OAc}$) were identified at δ 4.64 and 4.60. For the $GlcI^{3\text{-}OAc}$ spin system, with H-1 at δ 4.60, the chemical shift values were consistent with acetylation at O-3 as evidenced by downfield resonances obtained for H-2 (0.12 ppm), H-3 (1.47 ppm), H-4 (0.25 ppm), and C-3 (2.8 ppm), while the resonances for C-2 (−1.9 ppm) and C-4 (−2.9 ppm) were shifted upfield. For the $GlcI^{3\text{-}OAc}$ spin system, with H-1 at δ 4.64, downfield shifts were obtained for the signals from H-2 (0.09 ppm), H-3 (1.46 ppm), H-4 (0.22 ppm), and C-3 (2.8 ppm), while the resonances for C-2 (−1.9 ppm) and C-4 (−2.9 ppm) were shifted upfield. It is anticipated that the appearance of two spin systems of GlcI is due to the influence of HepI being acetylated to some degree.

Several anomeric signals for HepI and HepII were detected due to the microheterogeneity caused by the anhydro-forms of Kdo.[19] However, this heterogeneity was also caused by the presence of non-acetylated and monoacetylated HepI. While acetylation of HepI was indicated by CE-ESI-MS/MS, NMR analyses permitted the determination of the exact position of the *O*-acetyl group. Anomeric ^{1}H and ^{13}C signals corresponding to non-acetylated HepI were identified at δ 5.04/100.8, 5.10/1001.2, and 5.15/101.1. Two major spin systems corresponding to HepI with an acetylation site at O-2 were identified and their anomeric signals overlapped

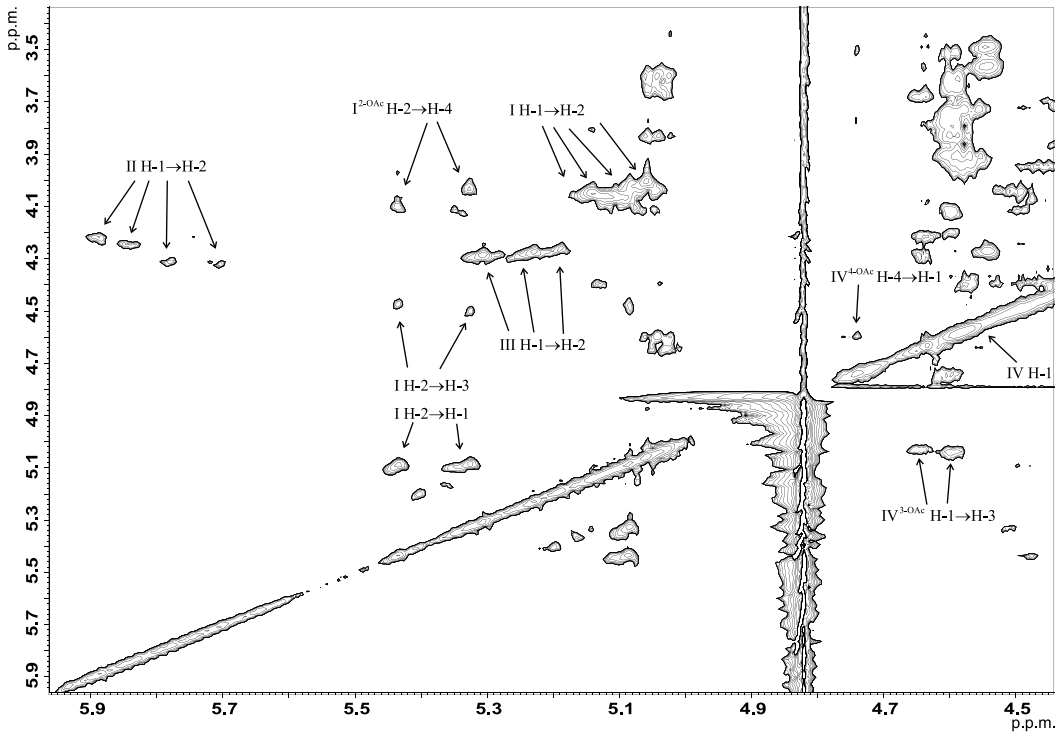

Figure 4. Selected region of the two-dimensional gradient and phase-sensitive TOCSY spectrum (spinlock time 180 ms) of OS derived from LPS of 723. Cross-peaks of significant importance are labeled. See Table 6 for an explanation of the roman numerals.

at δ 5.08/99.3. The position of the acetylation site was corroborated by the downfield ^{1}H chemical shifts of the H-2 resonances, and the COSY and NOESY spectra in which the H-1 signals had cross-peaks to the H-2 resonances at δ 5.33 (+1.33 ppm) and 5.44 (+1.44 ppm, Fig. 2), respectively. Additional minor spin systems belonging to monoacetylated HepI were identified at δ 5.19 and 5.16 since they had COSY cross-peaks to H-2 signals at 5.41 and 5.36, respectively. Several anomeric ^{1}H signals were detected for HepII at δ 5.90 (most abundant), 5.85 (minor), 5.79 (trace), and 5.72 (trace). NOESY cross-peaks were observed from the HepII anomers at δ 5.90 and 5.85 to the H-1 signals of HepIII at δ 5.31 and 5.24, respectively. NMR signals corresponding to H-2 and C-2 of both HepIII residues were recognized around 4.29 and 70.3 ppm, respectively. H-3 and C-3 were recognized at δ 4.32/74.3, altogether corresponding to non-acetylated sites. CE-MS data indicated that a minor proportion of HepIII was monoacetylated, however data supporting the exact position of an *O*-acetyl group could not be found. The phosphorylation pattern of *P*Etn, *P*EtnII, and *P*Cho was similar to that in the LPS-OH sample. This was corroborated by the ^{1}H–^{31}P HMQC spectrum, which showed the respective phosphorous atoms of *P*EtnI and *P*EtnII at δ 0.79 and −0.18 correlated to H-6 of HepII and H-3 of HepIII. The ^{1}H–^{31}P studies also showed that the phosphorous atom of *P*Cho coupled to all of the H-$6_{a,b}$ resonances indicated in Table 6.

From the combined data it could thus be concluded that the Hex1 glycoform of NTHi 723 has structure 3 in which an acetyl or glycine group can substitute the sugars of the core at any of the positions.

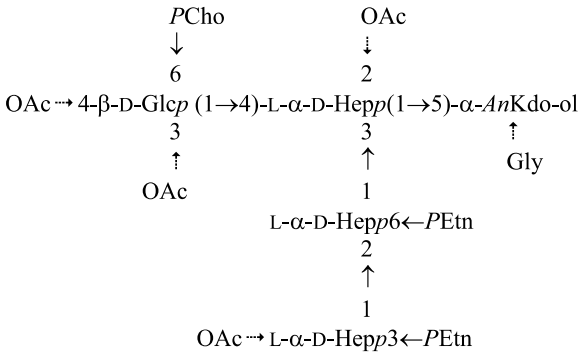

Structure 3

2.3.3. LPS-OH from 723-2. ESI-MS^{n} on permethylated and dephosphorylated OS from NTHi 723 revealed that in that preparation HepIII in a small population of glycoforms was substituted by a disaccharide epitope (see Table 4). In another batch of LPS referred to as 723-2, these glycoforms were found to be expressed to a much higher extent, which enabled us to investigate the identity of this epitope.

Sugar analysis of LPS-OH from 723-2 revealed D-glucose, D-galactose, D-GlcN, and L-*glycero*-D-*manno*-heptose (Table 1). Methylation analysis on the LPS-OH

material showed terminal Glc, terminal Gal, 4-substituted Glc, 6-substituted Glc, terminal Hep, 2-substituted Hep, 3-substituted Hep, 3,4-substituted Hep, 2,3-substituted Hep, and 6-substituted GlcN (Table 3). The higher presence of terminal Gal and 4-substituted Glc in this preparation indicated a D-Gal-(1→4)-D-Glc disaccharide as a possible terminal structure. The ESI-MS spectrum of LPS-OH from 723-2 showed ions corresponding to the same glycoforms as observed for NTHi 723 but with higher abundances of Hex 3 glycoforms (Table 2). Thus, for 723-2, abundant quadruply/triply charged ions were observed at *m*/*z* 569.4/759.2, 599.8/799.9, 630.6/840.9, 640.5/853.4, 680.9/908.1, and 711.5/949.1 corresponding to *P*Cho·Hex_1·Hep_3·*P*Etn_{1-3}·P_1·Kdo_1·LipidA-OH, *P*Cho·Hex_2·Hep_3·*P*Etn_2·P_1·Kdo_1·LipidA-OH, and *P*Cho·Hex_3·Hep_3·*P*Etn_{2-3}·P_1·Kdo_1·LipidA-OH, respectively.

NMR data indicated a heterogeneous mixture of glycoforms since several HepIII spin systems were observed in COSY, TOCSY, and NOESY spectra with H-1/H-2 cross-peaks at δ 5.10/4.30, 5.17/4.15, and 5.20/4.27. NOESY data indicated that the anomeric signals at δ 5.17 and 5.20 were from terminal HepIII residues since further couplings to a Glc or Gal residue were not detected. Anomeric resonances of HepI and HepII were identified at δ 5.04–5.07 and 5.80, respectively.

Three anomeric signals representing GlcI, GlcII, and GalI were observed at δ 4.53/103.9, 4.68/103.5, and 4.45/103.9. In addition, the anomeric signals of the α- and β-linked GlcN residues of the lipid A part were observed at δ 5.48 and 4.63, respectively. Chemical shift data were consistent with GlcI and GalI being terminal residues and GlcII being substituted in C-4 in agreement with methylation analysis. The occurrence of interresidue NOE between H-1 of GlcI and H-4/H-6 of HepI confirmed the 1,4 linkage between GlcI and HepI. Interresidue NOE connectivities between proton pairs GalI H-1/GlcII H-4 and GlcII H-1/HepIII H-1/H-2 established the sequence of a disaccharide unit and its attachment point to HepIII as β-D-Gal-(1→4)-β-D-Glc-(1→2 (Fig. 5). From the combined MS and NMR data from LPS of 723 and 723-2, it could thus be concluded that the Hex3 glycoform of NTHi 723 has structure 4.

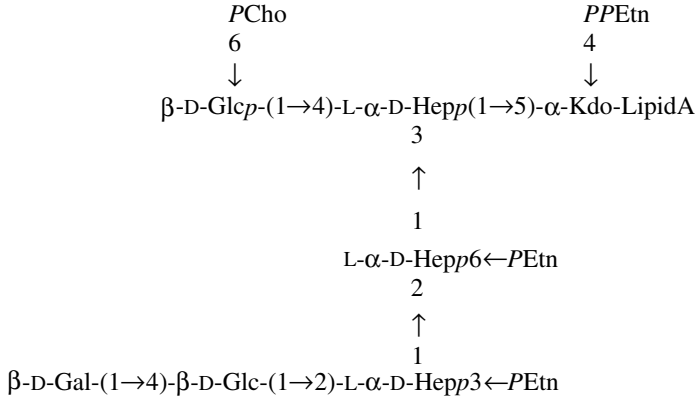

Structure 4

3. Discussion

Previous studies of LPS from *H. influenzae* have resulted in a structural model consisting of a conserved L-*glycero*-D-*manno*-heptose-containing trisaccharide inner core attached via a phosphorylated Kdo unit to the lipid A moiety. The results of this study confirmed the presence of this structural element in NTHi 723, and it also was found that this strain expresses LPS with glycose extensions from HepI and HepIII as indicated by tandem ESI-MS on dephosphorylated and permethylated oligosaccharide material. NMR analysis of the LPS-OH and oligosaccharide materials showed that HepI was substituted by a β-D-Glc residue and HepIII was substituted by the lactose epitope β-D-Gal*p*-(1→4)-β-D-Glc*p*-(1→2 and the truncated variant of it.

A characteristic feature of *H. influenzae* LPS is the extensive inter- and intra-strain heterogeneity of the oligosaccharide portion of the LPS due to phase variation. The potential repertoire of heterogeneous oligosaccharide glycoforms is key to the role of the LPS in both the commensal and disease-causing behavior of the bacterium. In the study presented here, detailed structural analysis of the oligosaccharide portion of NTHi 723 LPS not only confirmed the capacity for this strain to express a heterogeneous pattern of glycosylation but also of *O*-acetylation, *O*-glycylation, and phosphorylation by *P*Etn. Previous studies have shown that the inner- and outer-core regions of several *H. influenzae* strains are *O*-acetylated.[12–14,21,22] Interestingly, as indicated by CE-ESI-MS^n data on NTHi 723, it was found that the proximal and distal heptoses in the inner and the β-D-glucose in the outer core could be sites for *O*-acetylation. This is the first study to show that an *O*-acetyl group can substitute HepI in

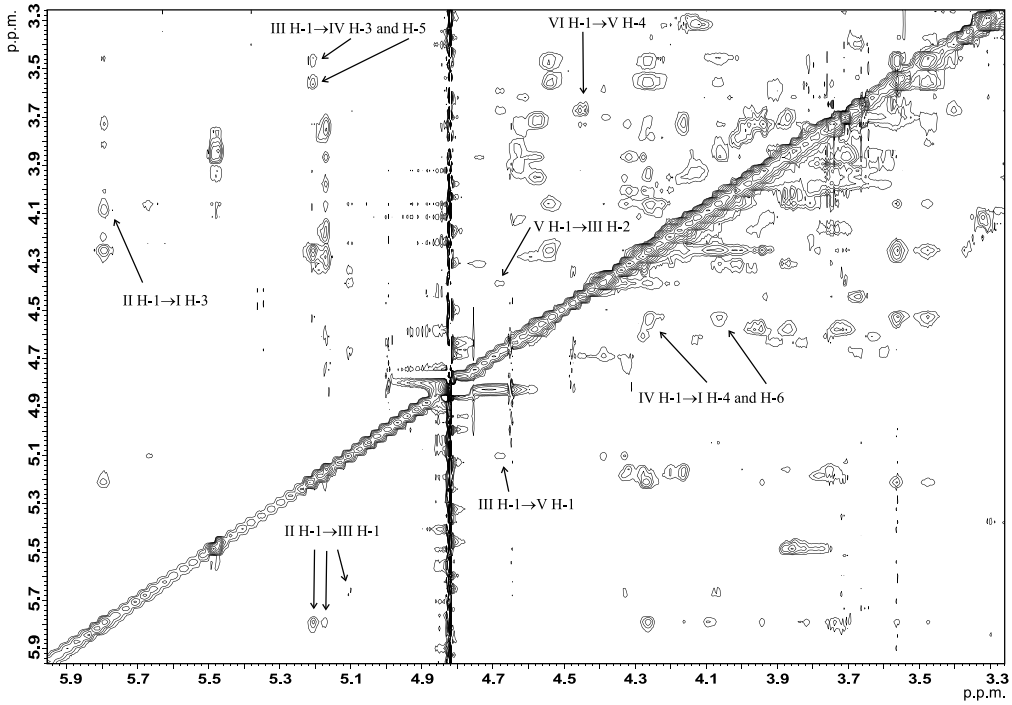

Figure 5. Selected region of the two-dimensional NOESY spectrum (mixing time 250 ms) of LPS-OH derived from LPS of NTHi 723-2. Cross-peaks of significant importance are labeled. See Table 5 for an explanation of the roman numerals.

H. influenzae LPS. NMR and other analyses of NTHi 723 provided unequivocal evidence that *O*-acetyl groups were linked to the HepI residue at C-2 position and to GlcI at C-3 or C-4 positions. However, it cannot be excluded that the two different acetylation sites on GlcI are caused by acetyl migration. Interestingly, this is the first study to show that the HepI can be substituted at the C-2 position by any substituents. Due to the heterogeneity of the oligosaccharide material, giving rise to weak and overlapping signals, the positions of the acetyl group on the HepIII residues were not determined.

Recently, it was that established the acetylase gene *OafA* is involved in the expression of an *O*-acetyl group from the distal heptose.[23] This also led to the observation that *O*-acetyl groups are involved in virulence. When the *OafA* was inactivated in NTHi 723, the resulting mutant 723*OafA* displayed a reduced resistance to the killing effect of normal human sera indicating that this epitope may have some biological relevance.[23] Thus, the complex pattern of *O*-acetylation seen in the LPS of strain NTHi 723 would be consistent with a role for the substituent in the behavior of the bacteria in different host compartments and microenvironments.

NTHi 723 as well as two other strains studied by our group, NTHI 981 and NTHi 1124, were shown to be highly substituted by *P*Etn located to the O-3 position of the HepIII residue.[6,24] The gene involved in adding *P*Etn to O-3 of HepIII is still unknown and is currently under investigation.

All *H. influenzae* strains investigated so far express minor amounts of the ester-linked amino acid glycine substituting the core region of *H. influenzae* LPS. The most common site for this substituent is HepIII, but it has also been found at HepII or Kdo. In NTHi 723, the position of glycine is indicated at Kdo by CE-ESI-MS. The biological significance of glycine on the role of LPS of *H. influenzae* has not been investigated in *H. influenzae* and the gene(s) required for its addition have not been identified.

4. Experimental

4.1. Bacterial growth and LPS preparation

NTHi 723 was obtained from the Finnish Otitis Media Study Group and is an isolate from the middle ear. LPS prepared from two batch growths of NTHi 723 was analyzed and referred to as 723 and 723-2, respectively. Bacteria were grown in brain–heart infusion broth supplemented with haemin (10 μg/ml) and NAD (2 μg/ml), and, for batch growth 723-2, Neu5Ac (10 μg/ml) was also added. LPS was extracted from lyophilized bacteria using phenol/chloroform/light petroleum as described previously but with the modification that the LPS was precipitated with 6 vol diethyl ether–acetone (1:5, by volume).[16] LPS was purified by ultracentrifugation (82,000*g*, 4 °C, 12 h).

4.2. Chromatography

Gel filtration chromatography was performed using a Bio-Gel P4 column (2.5 × 80 cm) with pyridinium acetate (0.1 M, pH 5.3) as eluent and a differential refractometer as detector.

4.3. Preparation of oligosaccharides

(a) *O-Deacylation of LPS with hydrazine*. *O*-Deacylation of LPS was achieved with anhydrous hydrazine as previously described.[25]

(b) *Mild acid hydrolysis of LPS.* Reduced core oligosaccharide (OS) material was obtained following mild acid hydrolysis of LPS (42 mg 723, 1% acetic acid, pH 3.1, 100 °C, 2 h). The reducing agent, borane-*N*-methylmorpholine complex (10.6 mg), was included in the hydrolysis mixture. The insoluble lipid A (12 mg) was separated from the hydrolysis mixtures by centrifugation. Following purification on the Biogel P4 column the oligosaccharide fraction (20 mg) was obtained.

(c) *Dephosphorylation.* Dephosphorylation of OS material was performed with 48% aqueous HF, as described previously.[24]

4.4. Mass spectrometry

GLC–MS was carried out with a Hewlett-Packard 6890 chromatograph connected to a Micromass quadrupole mass spectrometer using a DB-5 fused silica capillary column [25 m × 0.25 mm (0.25 μm i.d.)] and a temperature gradient of 130 °C (1 min)→250 °C at 3 °C/min.

Electrospray ionization mass spectrometry (ESI-MS) on LPS-OH and OS samples was recorded on a VG Quattro triple quadrupole mass spectrometer (Micromass, Manchester, UK) in the negative ion mode. The samples were dissolved in a mixture of water/acetonitrile (1:1, v/v). Sample solutions were injected via a syringe pump into a running solvent of water/acetonitrile (1:1, v/v) at a flow rate of 10 μl/min. The instrument was mass calibrated and tuned in the negative mode with a sugar mixture between *m*/*z* 250–1200 by using the supplied Masslynx software. Spectra were averaged over 20 scans with a scan speed of 6 s per scan. The spectra were digitally smoothed with a 2-point smoothing routine. Multiple step tandem ESI-MS (ESI-MS^n) experiments on permethylated OS samples were performed in the positive ion mode on a Finnigan LCQ iontrap mass spectrometer (Finnigan-MAT, San Jose, CA). Samples were dissolved in 1 mM sodium acetate in MeOH/water (7:1, v/v) at a flow rate of 10 μl/min. CE-ESI-MS^n was carried out with a Crystal model 310 CE instrument (ATI Unicam, Boston, MA, USA) coupled to an API 3000 mass spectrometer (Perkin–Elmer/Sciex, Concord, Canada) via a MicroIonspray interface as described previously.[15]

4.5. Analytical methods

Sugars were identified by GLC–MS as their alditol acetates or (+) 2-butyl acetylated glycosides as previously described.[26,27] Methylation was performed with methyl iodide in dimethylsulfoxide in the presence of lithium methylsulfinylmethanide.[28] The methylated compounds were recovered using a SepPak C18 cartridge and subjected to sugar analysis or ESI-MS^n. The relative proportions of the various alditol acetates and partially methylated alditol acetates obtained in sugar- and methylation analyses, discussed below, correspond to the detector response of the GLC–MS. Fatty acids were identified as previously described.[9]

4.6. NMR spectroscopy

NMR spectra were recorded in deuterium oxide (D_2O) at 22 °C and pD 6.2 (OS) or pD 8.0 (LPS-OH). *O*-Deacylated LPS (LPS-OH) samples were solubilized by adding perdeutero-EDTA (2 mM) and perdeutero-SDS (10 mg/ml) to the D_2O solution. Spectra were acquired on a JEOL 500 MHz spectrometer using standard pulse sequences. Chemical shifts were reported in parts per million, and referenced to external sodium 3-trimethylsilylpropanoate-d_4 (δ 0.00, ^{1}H), external acetone (δ 30.1, ^{13}C), and external trimethyl phosphate (δ 2.00, ^{31}P). ^{1}H,^{1}H-gradient selected correlated spectroscopy (gCOSY), gradient phase-sensitive selected total correlation spectroscopy (gTOCSY) with a spinlock time of 180 ms, gradient selected heteronuclear single quantum coherence (gHSQC), gradient selected heteronuclear multiple quantum coherence (gHMQC), and gradient selected heteronuclear multiple-bond correlation (gHMBC) experiments were performed according to standard pulse sequences. For inter-residue correlation, two-dimensional gradient selected nuclear Overhauser effect spectroscopy (gNOESY) experiments with a mixing time of 250 ms were used.

Acknowledgments

We thank the members of the Finnish Otitis Media Study group at the National Health Institute in Finland for the provision of NTHi strains from the nasopharynx, obtained as part of the Finnish Otitis Media Cohort study. Anna-Karin Karlsson is acknowledged for GC–MS and ESI-MS analysis of NTHi 723-2 samples. Derek W. Hood and E. Richard Moxon were funded by a Programme Grant from the Medical Research Council, UK. Gaynor Randle is acknowledged for help with bacterial culture.

References

1. Kimura, A.; Hansen, E. J. *Infect. Immun.* **1986**, *51*, 69–79.
2. Phillips, N. J.; Apicella, M. A.; Griffiss, J. M.; Gibson, B. W. *Biochemistry* **1992**, *31*, 4515–4526.
3. Risberg, A.; Masoud, H.; Martin, A.; Richards, J. C.; Moxon, E. R.; Schweda, E. K. *Eur. J. Biochem.* **1999**, *261*, 171–180.
4. Cox, A. D.; Hood, D. W.; Martin, A.; Makepeace, K. M.; Deadman, M. E.; Li, J.; Brisson, J. R.; Moxon, E. R.; Richards, J. C. *Eur. J. Biochem.* **2002**, *269*, 4009–4019.
5. Schweda, E. K.; Landerholm, M. K.; Li, J.; Richard Moxon, E.; Richards, J. C. *Carbohydr. Res.* **2003**, *338*, 2731–2744.
6. Månsson, M.; Hood, D. W.; Moxon, E. R.; Schweda, E. K. *Eur. J. Biochem.* **2003**, *270*, 2979–2991.
7. Yildirim, H. H.; Hood, D. W.; Moxon, E. R.; Schweda, E. K. *Eur. J. Biochem.* **2003**, *270*, 3153–3167.
8. Masoud, H.; Martin, A.; Thibault, P.; Moxon, E. R.; Richards, J. C. *Biochemistry* **2003**, *42*, 4463–4475.
9. Helander, I. M.; Lindner, B.; Brade, H.; Altmann, K.; Lindberg, A. A.; Rietschel, E. T.; Zähringer, U. *Eur. J. Biochem.* **1988**, *177*, 483–492.
10. Mikhail, I.; Yildirim, H. H.; Lindahl, E. C.; Schweda, E. K. *Anal. Biochem.* **2005**, *340*, 303–316.
11. Weiser, J. N.; Williams, A.; Moxon, E. R. *Infect. Immun.* **1990**, *58*, 3455–3457.
12. Månsson, M.; Bauer, S. H.; Hood, D. W.; Richards, J. C.; Moxon, E. R.; Schweda, E. K. *Eur. J. Biochem.* **2001**, *268*, 2148–2159.
13. Månsson, M.; Hood, D. W.; Li, J.; Richards, J. C.; Moxon, E. R.; Schweda, E. K. *Eur. J. Biochem.* **2002**, *269*, 808–818.
14. Månsson, M.; Hood, D. W.; Moxon, E. R.; Schweda, E. K. *Eur. J. Biochem.* **2003**, *270*, 610–624.
15. Schweda, E. K.; Li, J.; Moxon, E. R.; Richards, J. C. *Carbohydr. Res.* **2002**, *337*, 409–420.
16. Galanos, C.; Luderitz, O.; Westphal, O. *Eur. J. Biochem.* **1969**, *9*, 245–249.
17. Bauer, S. H.; Månsson, M.; Hood, D. W.; Richards, J. C.; Moxon, E. R.; Schweda, E. K. *Carbohydr. Res.* **2001**, *335*, 251–260.
18. Li, J.; Bauer, S. H. J.; Månsson, M.; Moxon, E. R.; Richards, J. C.; Schweda, E. K. H. *Glycobiology* **2001**, *11*, 1009–1015.
19. Schweda, E. K.; Hegedus, O. E.; Borrelli, S.; Lindberg, A. A.; Weiser, J. N.; Maskell, D. J.; Moxon, E. R. *Carbohydr. Res.* **1993**, *246*, 319–330.
20. Schweda, E. K.; Jansson, P. E.; Moxon, E. R.; Lindberg, A. A. *Carbohydr. Res.* **1995**, *272*, 213–224.
21. Schweda, E. K.; Brisson, J. R.; Alvelius, G.; Martin, A.; Weiser, J. N.; Hood, D. W.; Moxon, E. R.; Richards, J. C. *Eur. J. Biochem.* **2000**, *267*, 3902–3913.
22. Landerholm, M. K.; Li, J.; Richards, J. C.; Hood, D. W.; Moxon, E. R.; Schweda, E. K. *Eur. J. Biochem.* **2004**, *271*, 941–953.
23. Fox, K. L.; Yildirim, H. H.; Deadman, M. E.; Schweda, E. K. H.; Moxon, E. R.; Hood, D. W. *Mol. Microbiol.* **2005**, *58*, 207–216.
24. Yildirim, H. H.; Li, J.; Richards, J. C.; Hood, D. W.; Moxon, E. R.; Schweda, E. K. *Biochemistry* **2005**, *44*, 5207–5224.
25. Holst, O.; Brade, L.; Kosma, P.; Brade, H. *J. Bacteriol.* **1991**, *173*, 1862–1866.
26. Sawardeker, J. S.; Sloneker, J. H.; Jeanes, A. *Anal. Chem.* **1965**, *37*, 1602–1604.
27. Gerwig, G. J.; Kamerling, J. P.; Vliegenhart, J. F. G. *Carbohydr. Res.* **1979**, *77*, 1–7.
28. Blakeney, A. B.; Stone, B. A. *Carbohydr. Res.* **1985**, *140*, 319–324.